JOURNAL OF VIROLOGY, Mar. 1978, p. 888-896
0022-538X/78/0025-0888$02.00/0

Vol. 25, No. 3
Printed in U.S.A.

High-Molecular-Weight RNAs of AKR, NZB, and Wild Mouse Viruses and Avian Reticuloendotheliosis Virus All Have Similar Dimer Structures

WELCOME BENDER,[1] YUEH-HSIU CHIEN,[1] SISIR CHATTOPADHYAY,[2] PETER K. VOGT,[3] MURRAY B. GARDNER,[3] AND NORMAN DAVIDSON[1]*

Division of Biology and Department of Chemistry, California Institute of Technology, Pasadena, California 91125[1]; Pediatric Oncology Branch, National Cancer Institute, Bethesda, Maryland 20014[2]; and Department of Microbiology and Department of Pathology, University of Southern California School of Medicine, Los Angeles, California 90033[3]

Received for publication 20 October 1977

Several 50 to 70S tumor viral RNAs have previously been shown by electron microscopy to be dimers, with the two monomer subunits joined near their 5′ ends. Five additional naturally occurring type C RNA tumor viruses have now been examined: AKR, an endogenous murine ecotropic virus; NZB, an endogenous murine xenotropic virus; an ecotropic and an amphotropic virus isolated from a wild mouse; and the avian reticuloendotheliosis virus (REV). All five 50 to 70S RNAs have similar 5′-to-5′ dimer structures. Therefore, the observations support the hypothesis that the dimer linkage is a structural feature common to all type C mammalian viruses. REV is the first example of an avian virus with a clear 5′-to-5′ dimer linkage. All of the mammalian viral RNAs, but not REV, showed symmetrically placed loops in each subunit of the dimer. Possible molecular structures and biological functions of the dimer linkages and loops are discussed.

The first 50 to 70S RNA from a tumor virus to be studied by electron microscopy in this laboratory was that of the endogenous cat virus, RD-114. The RNA was observed to be a dimer of two monomer subunits, each 10 kilobases (kb) in length, and the two monomers were joined together close to their 5′ ends in a structure termed the dimer linkage structure (2, 23). The choice of RD-114 was a fortunate historical accident, in that the dimer linkage of RD-114 RNA is more stable to dissociation than most other viruses we have studied, and so the dimer structure is usually maintained under the partially denaturing conditions needed to extend the RNA for spreading in a basic protein film.

Subsequent studies demonstrated very similar RNA dimers for BKD, an endogenous baboon virus (24); for WoMV, a sarcoma virus complex isolated from a woolly monkey (24); for the Friend murine virus mixture (9); and for Moloney murine leukemia virus (MuLV) and two variants of Moloney sarcoma virus (MSV) (20, 25). The dimer linkage of BKD is as stable to dissociation as that of RD-114, but for all the other viruses the linkage is considerably less stable and can be preserved only by relatively mild denaturation conditions of spreading for electron microscopy; under these conditions, many RNA molecules are not fully extended and are difficult to interpret. Nevertheless, many dimers with the same general structural features as RD-114 are seen on the grids. By contrast, avian sarcoma virus (ASV) RNA (Prague C, Prague B, and B77 strains of ASV have been examined), treated with the same mild denaturation conditions, does not show any reproducible dimer structures (2).

It was of interest to examine the RNAs of other tumor viruses to see how universal the dimer structure is and to attempt to correlate the variations in secondary structure features of the RNAs with other differences among the viruses in their sequences or biological properties. The RNAs from four naturally occurring murine and one avian virus are described here; they all have the 5′-to-5′ dimer linkage.

MATERIALS AND METHODS

Virus. The AKR-L1 strain of ecotropic MuLV, originally isolated from a leukemic AKR mouse (13), was propagated on secondary NIH Swiss mouse embryo cells (8). NZB virus was originally isolated by treating a cell line (NZB-Q) derived from a New Zealand Black mouse embryo with 5-iododeoxyuridine (NZB-Q-IU-1) and then co-cultivating these cells with mink lung fibroblast cells (12, 17). The NZB virus used here was propagated on these mink cells, the CCL64 line (17). The wild mouse viruses were produced by cultured embryo cells from a wild mouse trapped near

Los Angeles, Calif. (strain no. 1504). The ecotropic MuLV viral strain (1504-E), which grows only on mouse cells, and the amphotropic MuLV viral strain (1504-A), which grows on species of origin and on other mammalian cells, were cloned by limiting dilutions of the original virus stock onto mouse, rabbit, mink, or human cells (5). Both wild mouse viruses were grown on SC-1 cells, a line obtained from a wild mouse embryo (11). Reticuloendotheliosis virus (REV) strain T (27) was propagated on quail embryo cells.

Preparation of viral RNA. Viruses were pelleted from the cell supernatant, in some cases banded in sucrose, and then extracted with phenol or phenol-sodium dodecyl sulfate as previously described (24). The RNA was sedimented through a sucrose gradient (10 to 30% in 0.1 M NaCl-0.01 M Tris-0.001 M EDTA), and the 50 to 70S peak was used for microscopy.

Electron microscopy. 50 to 70S viral RNA was treated with glyoxal (1 M glyoxal-0.01 M PO_4, pH 7.0) for various times, dialyzed, hybridized with simian virus 40 (SV40)-poly(dT), and spread from 40% formamide as previously described (2). Alternately, the treated RNA was hybridized to SV40-polydeoxybromouridine [poly(dBrU)] and spread from 50% or 55% formamide (25). Molecules were photographed and measured; the magnification was calibrated using the SV40 circles as internal length standards (SV40 contour length taken as 1.76 μm). RNA lengths were computed assuming 1 μm = 3.9 kb for glyoxal treatment of 1 h at 37°C or 30 min at 42°C (18), or 1 μm = 4.1 kb for glyoxal treatment of 30 min at 37°C or 1 h at 37°C in the presence of 0.1 M NaCl. A less stringent glyoxal treatment gives slightly less extended RNA molecules; the exact length conversion depends on the particular treatment and the particular RNA. This factor is thus impossible to calibrate accurately for the mild glyoxal reaction conditions used here. The second calibration factor quoted above was obtained for BKD viral RNA treated with glyoxal in the presence of 50 mM NaCl (9).

Denaturing gels. Molecular lengths of viral RNAs were measured by agarose gel electrophoresis in the presence of 5 mM CH_3HgOH as previously described (1), except that the EDTA in the ER buffer was reduced from 1 mM to 0.1 mM. We believe that the reduction in EDTA concentration decreases the rate of transport of the CH_3HgOH out of the gel as a negative CH_3Hg-EDTA complex. This should ensure that the slowly electrophoresing RNA is always in the presence of 5 mM CH_3HgOH.

T_m determinations. Aliquots of 50 to 70S viral RNA in 0.1 M NaCl-0.01 M Tris-1 mM EDTA (pH 7.5) were heated to various temperatures for 60 to 90 s and then chilled to 0°C. The samples were then subjected to electrophoresis on a nondenaturing agarose gel (0.8% agarose) in ER borate buffer (1). The gels were stained with ethidium bromide (0.1 μg/ml) and photographed, or sliced and counted.

RESULTS

Monomer molecular lengths. The RNAs of AKR virus, NZB virus, the ecotropic wild mouse virus, and REV each showed a single band on a denaturing CH_3HgOH gel with mobilities corresponding to estimated molecular lengths of 9.6, 9.5, 9.3, and 9.2 kb, respectively (Fig. 1). (Amphotropic wild mouse virus RNA was not available in sufficient quantity for gel electrophoresis.)

AKR virus. 50 to 70S RNA from AKR virus was treated with glyoxal (37°C, 30 min), dialyzed, mixed with SV40-poly(dBrU), and spread for microscopy from 50% formamide. Figure 2A shows a typical dimer molecule with both poly(A) ends hybridized to short poly(dBrU) tails on an SV40 DNA circle. The AKR dimer structure is shown schematically in Fig. 3 together with the structures of all the other viral RNA dimers studied here or previously. Like the other mammalian viral RNAs, AKR RNA has a 5'-to-5' dimer linkage and a loop near the middle of each monomer subunit. The lengths and positions of the various secondary structure features are given in Table 1.

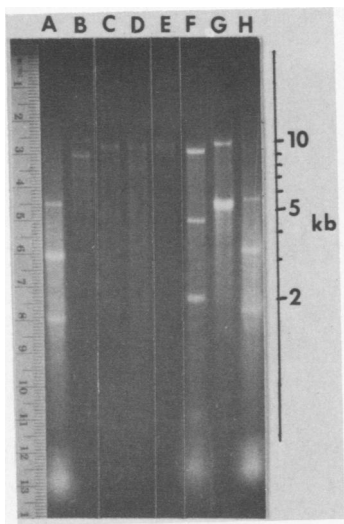

FIG. 1. *Molecular-weight determinations of viral RNAs on CH_3HgOH agarose gels. Lanes A and H contain molecular-weight standards which include Sindbis virus RNA, HeLa 28S ribosomal RNA, Escherichia coli 23S and 16S ribosomal RNAs, and E. coli tRNA (molecular lengths of 13.5, 5.5, 3.1, 1.7, and 0.1 kb, respectively). Lane B has Prague B ASV; the two bands are from transformation-competent and transformation-defective virions. Lane C has AKR RNA, lane D has NZB RNA, lane E has wild mouse ecotropic RNA, lane F has avian REV, and lane G has RNA from clone 3 Moloney MSV grown with Moloney MuLV as helper. All viral RNAs were 50 to 70S RNA selected after sucrose gradient sedimentation, except for the REV (lane F), which was total RNA extracted from pelleted virus. The REV RNA is contaminated with 18 and 28S ribosomal RNAs from the quail cells on which the virus was grown.*

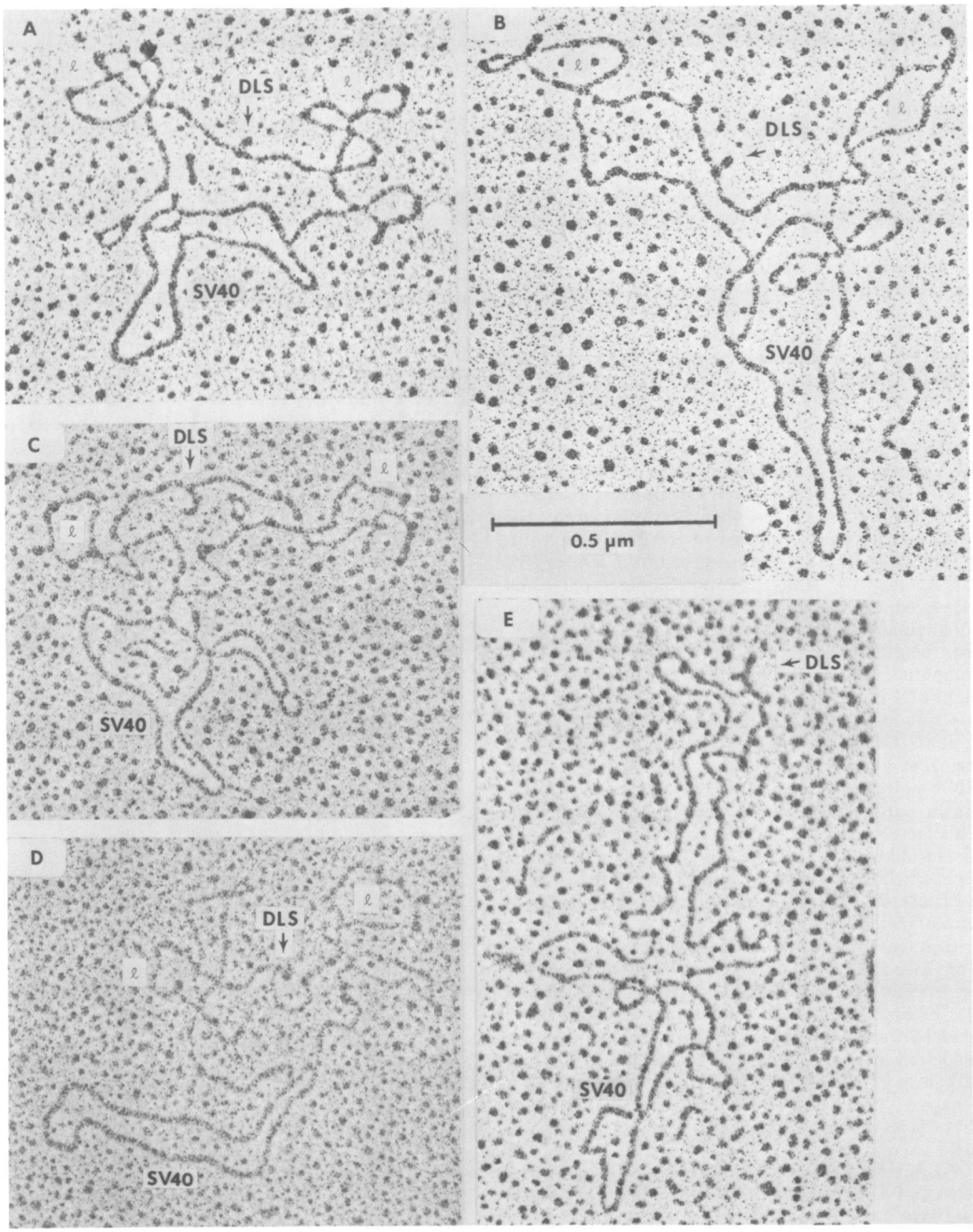

FIG. 2. *Electron micrographs of viral RNA dimers. All dimers are hybridized by their poly(A) tails to SV40 duplex circles with short tails of poly(T) or poly(dBrU). (A) AKR RNA; (B) NZB RNA; (C) wild mouse ecotropic viral RNA; (D) wild mouse amphotropic viral RNA; and (E) avian REV RNA. In (C), only one poly(A) end appears attached to the SV40. The dimer linkage structures are marked DLS, and the large loops are labeled l. All micrographs were printed at the same magnification.*

The large loops in the AKR monomers often had several crossover points that could be interpreted as the loop junction, especially if the RNA had been treated lightly with glyoxal (i.e., for 30 min instead of 1 h). A dimer with unusually many loop junctions is shown in Fig. 4A. For the diagram of Fig. 3, the average position for the loop junction is given, but the length

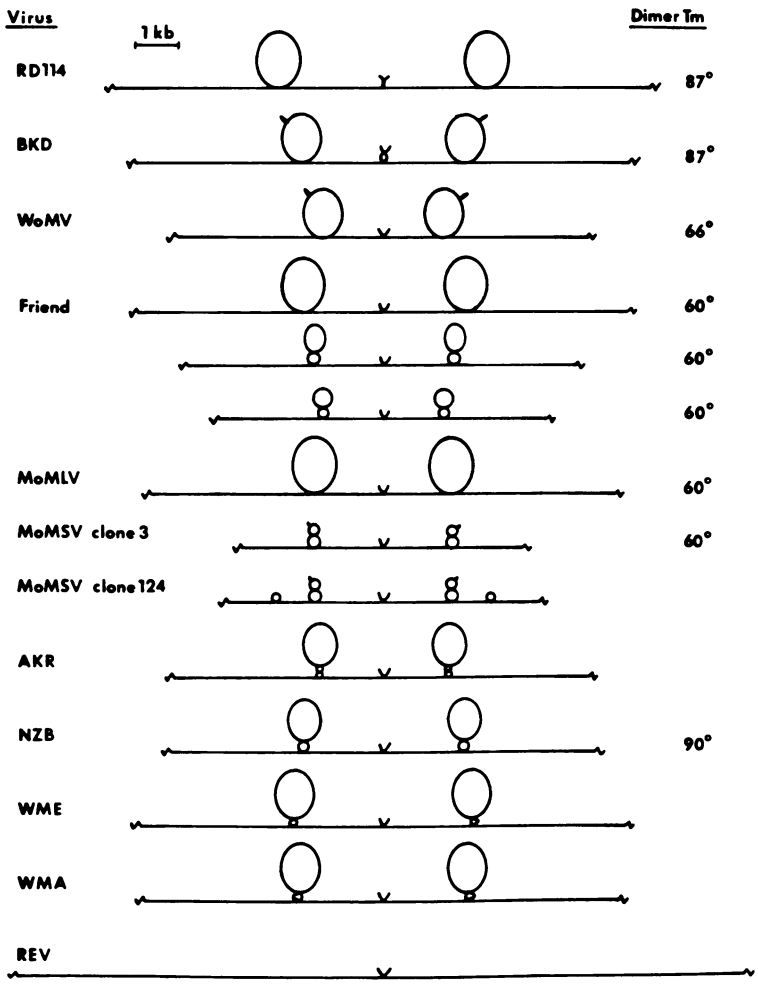

FIG. 3. *Diagram of the structures of all tumor virus RNA dimers so far examined in this laboratory. The dimer linkage structure is shown in the middle of each molecule; the zig-zag lines at the ends of the molecules symbolize poly(A). Next to each structure is listed the approximate melting temperature of the dimer linkage, where it has been determined. The viruses are: RD-114, the cat endogenous xenotrope (22); BKD, the baboon endogenous xenotrope (24); WoMV, the simian sarcoma virus complex (24); Friend murine virus complex, including the lymphatic leukemia virus and the spleen focus-forming virus (three different viral RNAs were present in the mixture studied) (7); MoMLV, the Moloney MuLV (20, 25); two isolates, clone 3 and clone 124 of MoMSV, Moloney murine sarcoma virus (20, 25); AKR murine endogenous ocotrope; NZB murine endogenous xenotrope; WME, a wild mouse ecotrope; WMA, a wild mouse amphotrope; and REV.*

measurements for this feature had very large standard deviations (see Table 1) which reflected these multiple or alternate loop junction points. The position of the midpoint in the loop, however, is a much more reproducible measurement (Table 1). Thus it appears that there are multiple pairs of sites that can be bound together, each pair being symmetrically placed relative to a fixed center point of the loop. Any one pair may or may not be joined in a particular molecule as mounted for electron microscopy.

NZB virus. The dimer linkage and the other secondary structure features of NZB dimers were much more stable to denaturation by glyoxal than those of any other murine viral RNA we examined. After treatment with glyoxal at 37°C for 30 min or 1 h, the 50 to 70S RNA molecules were mostly too condensed and tangled to interpret. Therefore, the NZB RNA was treated at higher temperature (0.5 h, 42°C) before spreading. A dimer molecule with both poly(A) ends hybridized to SV40-poly(dBrU) is shown in Fig. 2B. Even after the harsher glyoxal treatment, the RNA was still a dimer and showed somewhat more secondary structure, in the form of small loops and hairpins, than the

TABLE 1. *Contour lengths of viral RNA structural features (in kilobases)*

Virus[a]	Monomer length	Poly(A) to loop	Loop	Loop to DLS[b]	Loop midpoint to DLS
AKR	8.49 ±8%	3.39 ±17%	3.58 ±24%	1.64 ±30%	3.39 ±10%
NZB	8.67 ±7%	3.22 ±14%	3.44 ±18%	1.94 ±15%	3.68 ±6%
WME	9.29 ±8%	3.69 ±11%	3.88 ±16%	2.23 ±9%	4.17 ±8%
WMA	9.55 ±8%	3.68 ±14%	3.94 ±16%	2.03 ±9%	4.00 ±9%
REV	8.63 ±8%				

[a] WME, Wild mouse ecotropic; WMA, wild mouse amphotropic.
[b] DLS, Dimer linkage structure.

other murine viral RNAs. NZB RNA dimers had the large loops in each subunit, and, as in the loops in AKR RNA, there appeared to be multiple cohesive sites for loop formation, all defining approximately the same loop midpoint (Fig. 4B). The NZB dimer structure is diagramed in Fig. 3, and quantitative data on contour lengths are presented in Table 1.

Wild mouse virus. The RNAs of two different types of RNA tumor virus isolated from wild mice, designated ecotropic and amphotropic to indicate their host ranges, were also examined. The 50 to 70S RNA of each virus was spread for microscopy after treatment with glyoxal at 37°C for 1 h in the presence of 0.1 M NaCl. An example of each dimer is shown in Fig. 2. The monomer subunits of the dimer usually had the characteristic large loop. These loops did not show the multiple cohesion sites as seen in AKR or NZB, although they frequently had two pairing sites (see the left loop of Fig. 2C and the right loop of Fig. 2D) to form a small asymmetric loop at the base of the larger one. The wild mouse viral dimer structures are diagramed in Fig. 3, and measurements are included in Table 1.

REV. REV 50 to 70S RNA was treated with glyoxal (37°C, 30 min) and spread from 50% formamide. A dimer with both poly(A) ends attached to SV40-poly(dBrU) is shown in Fig. 2E. The monomer subunits frequently had small loops (about 1 kb in circumference) or short hairpins, but these features were not reproducible in position. In particular, there was no evidence of the larger symmetrical loops in each subunit as seen in all mammalian viruses.

Thermal melting of dimers. It was of interest to measure the temperature for dissociation of 50 to 70S ASV RNA into 35S subunits to see whether the lack of a reproducible dimer linkage in preparations for electron microscopy might be due to lower stability. ^{3}H-labeled 50 to 70S ASV RNA was heated briefly to various temperatures and then analyzed on a nondenaturing agarose gel. At 55°C, about 90% of the RNA still migrated as 50 to 70S; at 60°C, only about 40% was still 50 to 70S; and at 65°C, the RNA was 90% dissociated to 35S. This T_m of about 60°C is equivalent to those of Friend and Moloney viral RNAs (9, 25).

The NZB dimers were also examined because of their unexpected stability. Heating NZB RNA to 80°C did not affect the migration of 50 to 70S RNA, 90°C disrupted about half of the complexes, and 100°C disrupted them all. The approximate T_m of 90°C is about the same as those of RD-114 and BKD viral RNAs (22, 24).

The RNAs of AKR and the wild mouse viruses were not available in sufficient quantities to do such melts, but, for all three RNAs, the extent of denaturation seen by electron microscopy, after treatment with glyoxal or high concentrations of urea and formamide, was roughly equivalent to those seen for Friend or Moloney viral RNAs.

DISCUSSION

Figure 3 shows the basic structures of the high-molecular-weight RNAs of all mammalian RNA tumor viruses so far examined. RD-114 and BKD have 10 to 20% sequence homology to each other but not to any other virus in the list (19, 28). WoMV is not related to RD-114 or BKD, but has 15 to 20% sequence homology with several murine viruses (3). All murine viruses are partially related to each other, but the viruses of Fig. 3 are quite diverse in their degree of sequence homology. The ecotropic AKR virus and the xenotropic NZB virus both have about 50% sequence homology with Moloney MuLV (Y. Chien and S. Chattopadhyay, unpublished data). The defective spleen-sarcoma component of Friend virus is closely related to NZB but has only a little homology with the nondefective Friend lymphatic leukemia component for AKR virus (29). The RNAs from the three viruses, AKR, the wild mouse amphotrope, and the wild mouse ecotrope, are closely related but not identical by hybridization experiments; each hybridizes to a smaller extent (20 to 35%) with NZB (8; M. L. Bryant, P. Roy-Burman, M. B. Gardner, and B. K. Pal, personal communication).

In view of the sequence diversity of these mammalian viruses, the similarity in their structures is particularly striking. All nondefective viral RNAs have monomers of between 8 and 10

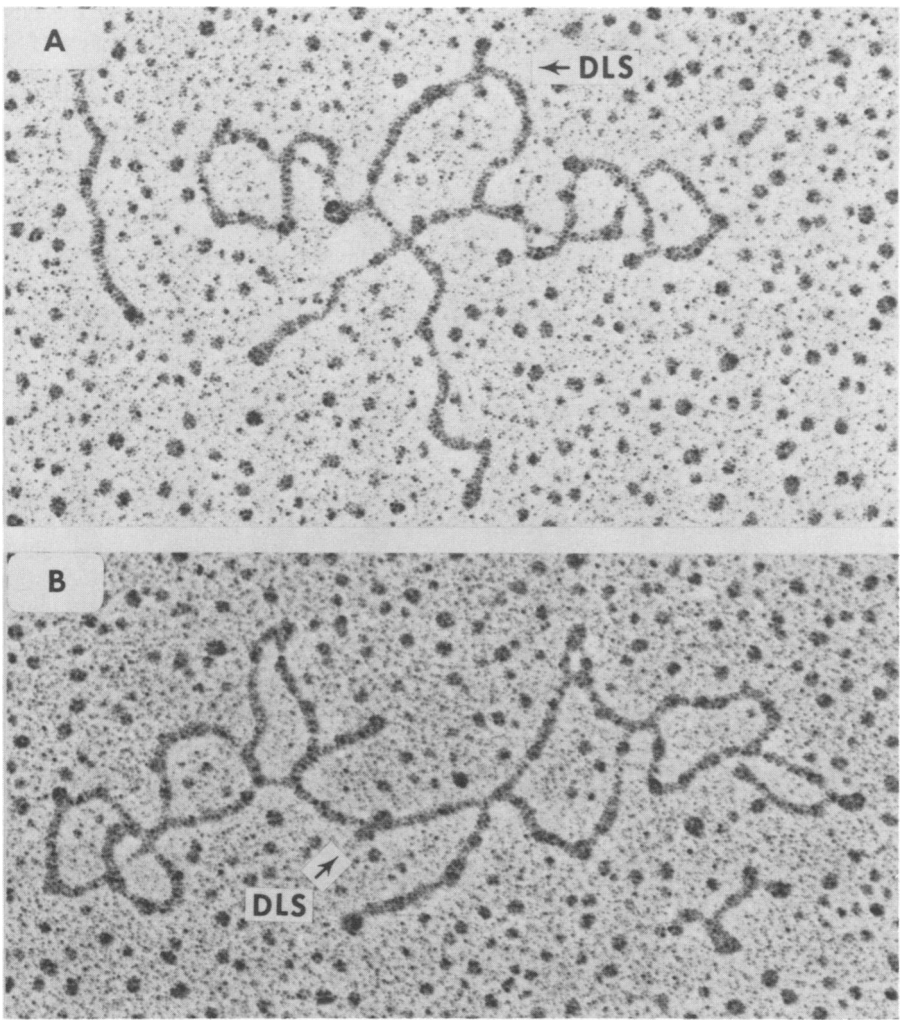

FIG. 4. *RNA dimers showing multiple pairings in each subunit. (A) AKR RNA; (B) NZB RNA. Both molecules have more possible pairing sites than average dimers, but such multiple pairings are common for both viruses. The dimer linkage structures (DLS) are indicated.*

kb; all have two monomers joined at their 5′ ends in a dimer linkage, and all have a large loop near the middle of each monomer subunit. The smaller defective viral RNAs retain the same basic structure, with proportionately smaller loops, although the distance from dimer linkage to the base of the loop is not greatly reduced in the small Friend and Moloney viral components.

The dimers of the nondefective mammalian viruses, however, are not identical in structure. They show minor differences in the several secondary structure features. There are large differences in the stability of the dimer linkage towards dissociation; the endogenous xenotropic viruses, RD-114, BKD, and NZB, all have a relatively stable dimer linkage with a T_m measured (or estimated from measurements in other solvents) as 85 to 90°C in 0.1 M Na^+ aqueous solvents. All of the other viruses we have studied are amphotropic or ecotropic, and, where measured, they have T_m's for dimer dissociation in the range of 60 to 70°C in aqueous solvents with 0.1 M Na^+.

In spite of the fact that B77 ASV dimers have about the same melting temperature (60°C) as do the several murine viruses (other than NZB) of Fig. 3, all of which have the characteristic 5′-to-5′ dimer structure, we have not been able to recognize any reproducible dimer linkage structure in the 50 to 70S RNA of the standard avian sarcoma viruses. On the other hand, REV, which belongs to a different family of avian viruses (21), does have a dimer structure, although it does not have the characteristic large loops.

Morphological and biochemical evidence indicates that REV is more closely related to mammalian viruses than to the standard avian sarcoma viruses (26, 30; E. Hunter, personal communication). Therefore, the available evidence is consistent with the hypothesis that the dimer linkage is a structural feature common to all mammalian type C oncornaviruses and to their close evolutionary relatives. We surmise that the same structure is present in the standard avian sarcoma viruses, but that it is slightly less stable and is obscured by other secondary structure features of the dimer RNA.

The general occurrence of the dimer structure of tumor viruses implies a biological function, but as yet the function is unknown. It seems probable to us that the structure of the 50 to 70S RNA is important for the copying of the RNA into DNA, since this happens quickly after penetration of the virus; stable 50 to 70S RNA does not reappear in the viral life cycle until after the virus buds off of the cell (6). Two monomers per virus might be required if reverse transcription proceeded by jumping from the 5′ end of one monomer to the 3′ end of another or if the initial DNA minus strand were a complete copy of one monomer plus a portion of the second monomer (i.e., slightly greater than the 10-kb unit length).

The physical nature of the dimer linkage is unknown. It is probable that a protein linker is not involved, since dimers are observed in RD-114 RNA extracted from virions by Pronase and sodium dodecyl sulfate treatment (22) and since incubation of purified MSV RNA dimers with proteinase K and sodium dodecyl sulfate does not change their thermal dissociation temperature (60°C, Fig. 3) (Y. H. Chien, personal communication). Several models for the dimer linkage, using only antiparallel base pairing, either directly between the two monomer RNA units or with a small nucleic acid linker, have been proposed (24). We calculate that a perfectly paired RNA duplex of only 10 to 15 base pairs (guanine + cytosine content, 50 mol%) would have a T_m of 60°C (the T_m of Moloney or Friend dimers), and 30 to 40 base pairs would melt at about 90°C (the T_m for RD-114, BKD, and NZB) (4, 16). It has been suggested from sequence information that the primer tRNA may be base-paired to both monomers and thus help to hold the dimer together (15). By measuring the size of the initial DNA transcript, the 3′ OH terminus of the primer is known to be bound to the RNA at 100 or 135 bases from the 5′ end for ASV or Moloney MuLV viruses, respectively (14). Figure 5 is a gallery of dimer linkage structures as found in several different tumor viruses. There is often considerable variation in appearance among examples on the same grid, presumably due to variation in the extent of glyoxal-induced denaturation. (The four examples of NZB are typical of the range of morphologies of the dimer linkage structure seen in murine viruses.) However, our general conclusion from examining many micrographs of the dimer linkages of RD-114 and BKD, and the most extended forms of the linkages seen with murine viruses and REV, is that the dimer linkage involves nucleotides extending at least 300 bases from the 5′ end of each monomer (Fig. 5). Therefore, we believe that viral RNA sequences on the 3′ side of the primer binding site are involved in the dimer linkage.

The loops near the middle of each monomer are also a reproducible feature in the mammalian RNA tumor viruses. The loops are not quite centered in the monomer; the midpoint of the loop is usually about 60% of the monomer length from the poly(A) end.

The molecular structure of the cohesive sites or sequences that cause loop formation is not known. The most obvious assumption is that they are due to base pairing between inverted repeat sequences, similar to the clover-leaf structure for tRNA and the base-paired secondary structure features proposed for other RNAs (10). However, the loop structures do not reform after thermal melting and cooling. They could be held together by proteins or by small RNA linker molecules, or perhaps there are RNA sequences base paired in the native dimer which, after melting, form alternate pairing arrangements.

In most murine viral RNAs, the base of the loop is held together at two or more points; this was most obvious for Friend virus (9) and for AKR and NZB as reported here. In BKD, the monomer RNA was often held together again between a point close to the 3′ end and one close to the 5′ end (24). In NZB, such multiple associations between the 3′ region and the 5′ region were often seen (as in Fig. 4B), although the junction points were not reproducible. This multiple pairing of the monomer with itself suggests that in the virion each monomer is folded back on itself. Such a configuration would bring the 3′ ends close to the dimer linkage, and transcription initiated at the primer near the 5′ end could then more easily jump to a 3′ end. Alternatively, or in addition, the loop structures we see could, if they also exist in viral mRNA, be important for translation control.

Finally, it is important to emphasize that the RNA molecules studied here have been partially denatured to extend them for microscopy. There are probably other associations in the virion, weaker than the dimer linkage or loop junctions, which are always disrupted by these techniques. Indeed, the absence of a dimer linkage structure

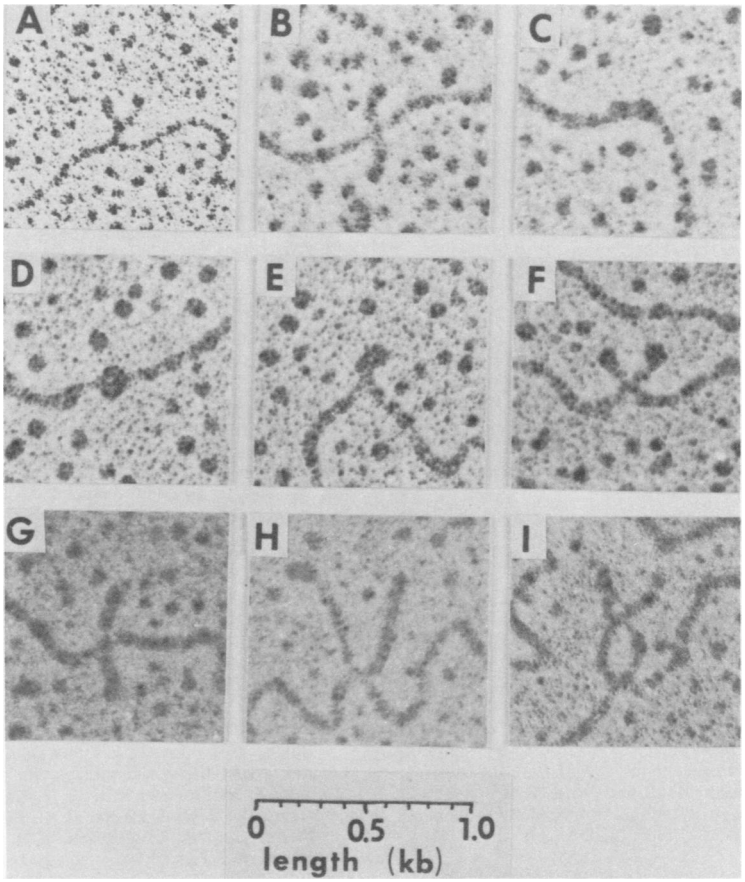

FIG. 5. *Gallery of dimer linkage structures. The dimer linkages are from RD-114 (A), REV (B), NZB (C–F), and BKD (G–I). The NZB structures (C–F) were all found on the same grid and were chosen to show the range of variation typically seen in all the murine viruses studied. The Y-shaped linkage (A) is distinctive to RD-114, and BKD (G–I) apparently has two linkage sites, either one or both of which may be paired in any individual dimer.*

in ASV may be because the structure is slightly more sensitive to glyoxal than those of mammalian viruses. A more detailed picture of the native structure of viral RNA may possibly be obtained by chemically or photochemically cross-linking the RNA in the virion, extracting and spreading the RNA for electron microscopy under highly denaturing conditions, and then systematically mapping the points of cross-linking.

ACKNOWLEDGMENTS

We thank Marilyn R. Lander and Wallace P. Rowe of the National Institute of Allergy and Infectious Diseases for assistance and advice.

W.B. has been the recipient of a National Science Foundation fellowship and of a Public Health Service training grant from the National Institute of General Medical Sciences. This research has been supported by Public Health Service contracts NO1-CP-43306 and NO1-CP-53500 with the Virus Cancer Program of the National Cancer Institute. Y.C. has been supported by Public Health Service postdoctoral fellowship no. 5-F32-CA-05099 from the National Cancer Institute.

LITERATURE CITED

1. **Bailey, J. M., and N. Davidson.** 1976. Methylmercury as a reversible denaturing agent for agarose gel electrophoresis. Anal. Biochem. **70**:75–85.
2. **Bender, W., and N. Davidson.** 1976. Mapping of poly(A) sequences in the electron microscope reveals unusual structure of type C oncornavirus RNA molecules. Cell **7**:595–607.
3. **Benveniste, R. E., and G. J. Todaro.** 1973. Homology between type-C viruses of various species as determined by molecular hybridization. Proc. Natl. Acad. Sci. U.S.A. **70**:3316–3320.
4. **Billeter, M. A., C. Weissmann, and R. C. Warner.** 1966. Replication of viral ribonucleic acid. IX. Properties of double-stranded RNA from *Escherichia coli* infected with bacteriophage MS2. J. Mol. Biol. **17**:145–173.
5. **Bryant, M. L., and V. Klement.** 1976. Clonal heterogeneity of wild mouse leukemia viruses: host range and antigenicity. Virology **73**:532–536.
6. **Canaani, E., K. V. D. Helm, and P. Duesberg.** 1973. Evidence for 30–40S RNA as precursor of the 60–70S RNA of Rouse sarcoma virus. Proc. Natl. Acad. Sci. U.S.A. **70**:401–405.
7. **Chattopadhyay, S., M. R. Lender, D. S. Kramer, J.**

W. Hartley, A. S. Levine, and W. P. Rowe. 1977. The use of nucleic acid hybridization to demonstrate relatedness between the naturally occurring and laboratory strains of murine C-type viruses. *In* D. S. Yohn and P. Bentvelzen (ed.), Proceedings of the Eighth International Symposium on Comparative Research on Leukemia and Related Diseases. Elsevier, Amsterdam.

8. **Chattopadhyay, S. K., D. R. Lowy, N. M. Teich, A. S. Levine, and W. P. Rowe.** 1974. Qualitative and quantitative studies of AKR-type murine leukemia virus sequences in mouse DNA. Cold Spring Harbor Symp. Quant. Biol. **39**:1085–1101.
9. **Dube, S., H.-J. Kung, W. Bender, N. Davidson, and W. Ostertag.** 1976. Size, subunit composition, and secondary structure of the Friend virus genome. J. Virol. **20**:264–272.
10. **Fiers, W., R. Contreras, F. Duerinck, G. Haegeman, D. Iserentant, J. Merregaert, W. Min Jou, F. Molemans, A. Raeymaekers, A. VanderBerghe, G. Volchkaert, and M. Ysebaert.** 1976. Complete nucleotide sequence of bacteriophage MS2 RNA: primary and secondary structure of the replicase gene. Nature (London) **260**:500–507.
11. **Hartley, J. W., and W. P. Rowe.** 1975. Clonal cell lines from a feral mouse embryo which lack host-range restrictions for murine leukemia viruses. Virology **65**:128–134.
12. **Hartley, J. W., and W. P. Rowe.** 1976. Naturally occurring murine leukemia viruses in wild mice: characterization of a new "amphotropic" class. J. Virol. **19**:19–25.
13. **Hartley, J. W., W. P. Rowe, and R. J. Huebner.** 1970. Host-range restrictions of murine leukemia viruses in mouse embryo cell cultures. J. Virol. **5**:221–225.
14. **Haseltine, W. A., D. G. Kleid, A. Panet, E. Rothenberg, and D. Baltimore.** 1976. Ordered transcription of RNA tumor virus genomes. J. Mol. Biol. **106**:109–131.
15. **Haseltine, W. A., A. M. Maxam, and W. Gilbert.** 1977. Rous sarcoma virus genome is terminally redundant: the 5′ sequence. Proc. Natl. Acad. Sci. U.S.A. **74**:989–993.
16. **Hayes, F. N., E. H. Lilly, R. L. Ratliff, D. A. Smith, and D. L. Williams.** 1970. Thermal transitions in mixtures of polydeoxyribonucleotides. Biopolymers **9**:1105–1117.
17. **Henderson, I. C., M. M. Lieber, and G. J. Todaro.** 1974. Mink cell line Mv-1Lu (CCL 64). Focus formation and generation of "nonproducer" transformed cell lines with murine and feline sarcoma viruses. Virology **60**:282–287.
18. **Hsu, M. T., H.-J. Kung, and N. Davidson.** 1973. An electron microscope study of Sindbis virus RNA. Cold Spring Harbor Symp. Quant. Biol. **38**:943–950.
19. **Hu, S., N. Davidson, M. Nicolson, and R. M. McAllister.** 1977. Heteroduplex study of the sequence relations between RD-114 and baboon viral RNAs. J. Virol. **23**:345–352.
20. **Hu, S., N. Davidson, and I. M. Verma.** 1977. A heteroduplex study of the sequence relationships between the RNAs of M-MSV and M-MLV. Cell **10**:469–477.
21. **Kang, C.-Y., and H. M. Temin.** 1973. Lack of sequence homology among RNAs of avian leukosis-sarcoma viruses, reticuloendotheliosis viruses, and chicken endogenous RNA-directed DNA polymerase activity. J. Virol. **12**:1314–1324.
22. **Kung, H.-J., J. M. Bailey, N. Davidson, M. O. Nicolson, and R. M. McAllister.** 1975. Structure, subunit composition, and molecular weight of RD-114 RNA. J. Virol. **16**:397–411.
23. **Kung, H.-J., J. M. Bailey, N. Davidson, P. K. Vogt, M. O. Nicolson, and R. M. McAllister.** 1974. Electron microscope studies of tumor virus RNA. Cold Spring Harbor Symp. Quant. Biol. **39**:827–834.
24. **Kung, H.-J., S. Hu, W. Bender, J. Bailey, N. Davidson, M. O. Nicolson, and R. M. McAllister.** 1976. RD-114, baboon and woolly monkey viral RNAs compared in size and structure. Cell **7**:609–620.
25. **Maisel, J., W. Bender, S. Hu, P. H, Duesberg, and N. Davidson.** 1977. Structure of 50 to 70S RNA from Moloney sarcoma viruses. J. Virol. **25**:348–394.
26. **Moelling, K., H. Gelderblom, G. Pauli, R. Friis, and H. Bauer.** 1976. A comparative study of the avian reticuloendotheliosis virus: relationship to murine leukemia virus and viruses of the avian sarcoma-leukosis complex. Virology **65**:546–557.
27. **Theilen, G. H., R. F. Ziegel, and M. J. Twiehaus.** 1966. Biological studies with RE virus (strain T) that induces reticuloendotheliosis in turkeys, chickens, and Japanese quail. J. Natl. Cancer Inst. **37**:731–743.
28. **Todaro, G. J., C. J. Sherr, R. E. Benveniste, M. M. Lieber, and J. L. Melnick.** 1974. Type C virus of baboons: isolation from normal cell cultures. Cell **2**:55–61.
29. **Troxler, D. H., J. K. Boyars, W. P. Parks, and E. M. Scolnick.** 1977. Friend strain of spleen focus-forming virus: a recombinant between mouse type C ecotropic viral sequences and sequences related to xenotropic virus. J. Virol. **22**:361–372.
30. **Ziegel, R. F., G. H. Theilen, and M. J. Twiehaus.** 1966. Electron microscopic observations on RE virus (strain T) that induces reticuloendotheliosis in turkeys, chickens, and Japanese quail. J. Natl. Cancer Inst. **37**:709–729.